Inorg. Chem. **2002**, *41*, 6875–6886

Copper(I) Halide Complexes with 1,3-Propanebis(diphenylphosphine) and Heterocyclic Thione Ligands: Crystal and Electronic Structures (DFT) of [CuCl(pymtH)(dppp)], [CuBr(pymtH)(dppp)], and [Cu(μ-I)(dppp)]$_2$

Paraskevas Aslanidis,*,† Philip J. Cox,‡,§ Savvas Divanidis,† and Athanassios C. Tsipis†

Inorganic Chemistry Laboratory, Faculty of Chemistry, Aristotle University of Thessaloniki, P.O. Box 135, GR-541 24, Thessaloniki, Greece, and School of Pharmacy, The Robert Gordon University, Schoolhill, Aberdeen AB 10 1FR, Scotland

Received July 24, 2002

Reaction of copper(I) chloride or bromide with equimolar amounts of the diphos ligand 1,3-propanebis(diphenylphosphine) and a heterocyclic thione (L) in acetonitrile/methanol solvent afforded mononuclear complexes of the type [CuX(dppp)(L)] with the diphosphine ligand acting as a chelating ligand. In contrast, copper(I) iodide under the same conditions gave the dimeric complex [Cu(μ-I)(dppp)]$_2$, which contains doubly bridging iodo ligands. The structures of three complexes, namely, [CuCl(pymtH)(dppp)], [CuCl(pymtH)(dppp)], and [Cu(μ-I)(dppp)]$_2$, have been established by single-crystal X-ray diffraction. Density functional calculations at the B3LYP level of theory provided a satisfactory description of the structural, bonding, electronic, and related properties of the [CuX(PH$_3$)$_2$] and [CuX(1,3-pdp)] (1,3-pdp = 1,3-propane-di-phosphine) complexes and their dimers along with their associations with the pyrimidine-2-thione (pymtH) ligand. The interaction of the pymtH ligand with the Cu(I) metal center in these complexes corresponds to loose associations, the computed interaction energies predicted to be about 20 kcal/mol for all complexes in the series. The bonding mechanism of the thione ligand with the Cu(I) metal centers involves both a σ-dative and π-back-bonding components. The coordination of the pymtH ligand is further stabilized by X···H–N bond formation being more pronounced in the chloro than in the iodo derivatives. The Cu–X bond was also found to be a composite bond involving σ- and π-dative bonding components. Most important is the presence of π-type MOs delocalized over the entire four-membered Cu(μ-X)$_2$Cu ring, which supports a ring current and could probably account for the nearly equivalent Cu–X bonds in the rhombus. Moreover, all [Cu(μ-X)(PH$_3$)$_2$]$_2$ dimers exhibit a σ-type MO corresponding to weak Cu···Cu interactions supporting through-ring intermetallic interactions, which seems to be responsible for the stabilization of the otherwise unstable antiaromatic Cu(μ-X)$_2$Cu ring.

Introduction

Owing to their relevance in biological systems, heterocyclic thiones have attracted considerable interest as ligands in metal complexes.[1] Because of their application in catalytic functions, transition metal complexes with phosphine ligands have also been studied extensively.[2] In a series of studies[3] we have explored the mixed-ligand copper(I) halide complexes blending both heterocyclic thione and tertiary arylphosphine ligands. In these complexes, the neutral thione molecules presenting both nitrogen and sulfur as potentially donating atoms always adopt the monodentate coordination mode binding the metal centers exclusively through the exocyclic sulfur atom in either a terminal or bridging mode. Nonetheless, a remarkable variety of structures ranging from mononuclear three- or four-coordinate species with trigonal planar and tetrahedral Cu(I), respectively, to double bridged dimers with asymmetric Cu(μ-S)$_2$Cu or Cu(μ-X)$_2$Cu units and a pseudotetrahedral geometry were obtained even within

* Author to whom correspondence should be addressed. E-mail: aslanidi@chem.auth.gr. Fax: +30 31 /997738.
† Aristotle University of Thessaloniki.
‡ The Robert Gordon University.
§ E-mail: p.j.cox@rgu.ac.uk.

(1) Raper, E. E. *Coord. Chem. Rev.* **1994**, *129*, 91−156.

(2) (a) Cotton, F. A.; Dunbar, K. R.; Verbruggen, M. G. *J. Am. Chem. Soc.* **1987**, *109*, 5498−5506. (b) Puddephatt, R. J. *Chem. Soc. Rev.* **1983**, *12*, 99. (c) Kiress, R. V.; Eisenberg, R. *Inorg. Chem.* **1989** *28*, 3372−3378.

10.1021/ic025896i CCC: $22.00
Published on Web 11/20/2002

a closely related series of thione ligands. In the course of our investigations we extensively discussed the factors which affect the stoichiometric and structural preferences of these complexes. Although the interplay of several parameters like the steric and electronic requirements of ligands and the geometrical flexibility on the part of the metal ion make structural prediction of these complexes extremely difficult, we found that steric demands of the phosphine ligands are likely to be the main factor that determines the coordination number of the metal. In the case of monomers, for example, triphenylphosphine but also tri-*m*- and tri-*p*-tolylphosphine always form four-coordinate complexes with the general formula $[CuX(PR_3)_2(thione)]$, whereas the steric demands of the *o*-methyl groups clearly favor three-coordination in the copper(I) halide complexes of tri-*o*-tolylphosphine.[3d,e] On the other hand, the question why two different types of binuclear copper(I) halide complexes of general formula $[CuX(PR_3)(thione)]_2$ exist involving either a double halide or a double thione-sulfur bridge is still waiting to be answered. On the basis of our earlier observations on a series of dimers, the coordination behavior (terminal or bridging mode) of each ligand has been supposed to depend on the nature of the halide ligand. In particular, formation of halide bridges has been found to be favored for the "soft" iodide but not for the "harder" chloride ligands,[4] whereas both bridging and terminal bonding modes were observed for the bromide ligands[5] since bromide lies on the borderline between soft and hard bases. However, the information obtained so far is not enough to establish the above supposition. To obtain a deeper insight into this very interesting field of research we have recently initiated a comparative investigation on substituting the unidentate triarylphosphines with bulkier multidentate phosphine ligands starting with acyclic bidentate phosphines of various chain lengths. At first attempt we used 1,2-bis(diphenylphosphino)ethane in an attempt to isolate chelated products, but this bidentate diphosphine ligand appeared to be insufficient to span tetrahedral positions, and it was not possible to isolate any mononuclear complexes.[6] In this work we report on the synthesis of a series of the copper(I) halide complexes formed upon reacting copper(I) halides with 1,3-propanebis(diphenylphosphine) (dppp) and a variety of heterocyclic thione ligands, as well as the structures of [CuCl(pymtH)(dppp)], [CuBr(pymtH)(dppp)], and $[Cu(\mu\text{-}I)(dppp)]_2$. Furthermore, to explore the electronic factors tuning the striking differences in the coordination behavior between the copper(I) halides, we performed DFT computational studies pursuing a 3-fold objective: (i) the determination of the structural, electronic, bonding, and related properties of the complexes, (ii) the understanding of the bonding mechanism of the coordination of the pymtH ligand with Cu(I) metal centers, and (iii) the exploration of the dimer formation only in the case of the iodide derivatives.

Experimental Section

Materials and Instruments. Copper(I) chloride, copper(I) bromide, copper(I) iodide, 1,3-bis(diphenylphosphino)propane, and all solvents are commercially available and were used as obtained, while the thiones (Merck or Aldrich) were recrystallized from hot ethanol prior to their use. IR, UV, and ^{1}H NMR spectra, conductivities, melting points, and elemental analyses of carbon, nitrogen, and hydrogen were performed as described previously.[3b]

Computational Details. The structural, electronic, and energetic properties of all compounds were computed at the Becke's 3-parameter hybrid functional[7] combined with the Lee−Yang−Parr correlation functional[8] level of theory, abbreviated as B3LYP, using the SDD basis set that includes Dunning/Huzinaga full double-ζ on the first row and Stuttgart/Dresden ECP's on the copper, phosphorus, and halogen atoms. The hybrid B3LYP functional was used, since it gives acceptable results for molecular energies and geometries, as well as proton donation, and weak and strong H-bonds.[9] In all computations no constraints were imposed on the geometry. Full geometry optimization was performed for each structure using Schlegel's analytical gradient method,[10] and the attainment of the energy minimum was verified by calculating the vibrational frequencies that result in absence of imaginary eigenvalues. All the stationary points have been identified for minimum (number of imaginary frequencies NIMAG = 0) or transition states (NIMAG = 1). All calculations were performed using the GAUSSIAN98 series of programs.[11] Moreover, the qualitative concepts and the graphs derived from the Chem3D program suite[12] highlight the basic interactions resulted from the DFT calculations.

(3) (a) Lecomte, C.; Skoulika, S.; Aslanidis, P.; Karagiannidis, P.; Papastefanou, S. *Polyhedron* **1989**, *8*, 1103−1109. (b) Karagiannidis, P.; Hadjikakou, S. K.; Aslanidis, P.; Hountas, A. *Inorg. Chim. Acta* **1990**, *178*, 27−34. (c) Karagiannidis, P.; Aslanidis, P.; Papastefanou, S.; Mentzafos, D.; Hountas, A.; Terzis, A. *Polyhedron* **1990**, *9*, 981−986. (d) Hadjikakou, S. K.; Aslanidis, P.; Karagiannidis, P.; Mentzafos, D.; Terzis, A. *Inorg. Chim. Acta* **1991**, *186*, 199−204. (e) Hadjikakou, S. K.; Aslanidis, P.; Karagiannidis, P.; Aubry, A.; Skoulika, S. *Inorg. Chim. Acta* **1992**, *193*, 129−135. (f) Aslanidis, P.; Hadjikakou, S. K.; Karagiannidis, P.; Gdaniec, M.; Kosturkiewicz, Z. *Polyhedron* **1993**, *12*, 2221−2226. (g) Aslanidis, P.; Hadjikakou, S. K.; Karagiannidis, P.; Kojic-Prodic B.; Luic, M.; *Polyhedron* **1994**, *13*, 3119−3125.

(4) (a) Hadjikakou, S. K.; Aslanidis, P.; Karagiannidis, P.; Mentzafos D.;. Terzis, A. *Polyhedron* **1991**, *10*, 935−940. (b) Hadjikakou, S. K.; Aslanidis, P.; Karagiannidis, P.; Hountas, A.; Terzis, A. *Inorg. Chim. Acta* **1991**, *184*, 161−166.

(5) (a) Karagiannidis, P.; Aslanidis, P.; Kessissoglou, D. P.; Krebs, B.; Dartmann, M. *Inorg. Chim. Acta* **1989**, *156*, 47−56. (b) Lecomte, C.; Skoulika, S.; Aslanidis, P.; Karagiannidis P.; Papastefanou, S. *Polyhedron* **1989**, *8*, 1103−1109.

(6) Cox, P. J.; Aslanidis, P.; Karagiannidis, P. *Polyhedron* **2000**, *19*, 1615−1620.

(7) (a) Becke, A. D. *J. Chem. Phys*. **1992**, *96*, 2155−2160. (b) Becke, A. D. *J. Chem. Phys*. **1993**, *98*, 5648−5652.

(8) Lee, C.; Yang, W.; Parr, R. G. *Phys. Rev*. **1988**, *B37*, 785.

(9) (a) Nicholas, J. B. *Top. Catal*. **1997**, *4*, 157. (b) Koch, W. R.; Hertwing, H. *Chem. Phys. Lett*. **1997**, *186*, 345−351. (c) Curtis, L. A.; Raghavachari, K.; Redfern, P. C.; Pople, *J. A. Chem. Phys. Lett*. **1997**, *270*, 419−426. (d) Smith, D. M.; Golding, B. T.; Radom, L. *J. Am. Chem. Soc*. **1999**, *121*, 9388−9399. (e) Ghandra, A. K.; Nguyen, M. T. *Chem. Phys*. **1998**, *232*, 299−306. (f) Nicholas, J. B. *Top. Catal*. **1999**, *9*, 181. (g) Arnaud, R.; Adamo, C.; Cossi, M.; Millet, A.; Vallé, Y.; Barone, V. *J. Am. Chem. Soc*. **2000**, *122*, 324−330.

(10) Schlegel, H. B. *J. Comput. Chem*. **1982**, *3*, 214.

(11) Frisch, M. J.; Trucks, G. W.; Schlegel, H. B.; Scusseria, G. E.; Robb, M. A.; Cheeseman, J. R.; Zakrzewski, V. G.; Montgomery, J. A.; Stratmann, R. E.; Burant, J. C.; Dapprich, S.; Millan, J. M.; Daniels, A. D.; Kudin, K. N.; Strain, M. C.; Farkas, O.; Tomasi, J.; Barone, V.; Cossi, M.; Cammi, R.; Mennucci, B.; Pomelli, C.; Adamo, C.; Clifford, S.; Orchterski, J.; Petersson, G. A.; Ayala, P. Y.; Cui, Q.; Morokuma, K.; Malick, D K.; Rabuck, A. D.; Raghavachari, K.; Foresman, J. B.; Cioslowski, J.; Ortiz, J. V.; Stefanov, B. B.; Liu, G.; Liashenko, A., Piskorz, P., Komaroni, I.; Gomperts, R.; Martin, R. L.; Fox, D. J.; Keith, T.; Al-Laham, M. A.; Peng, C. Y.; Nanayakkara, A.; Gonzalez, C.; Challacombe, M.; Gill, P. M.; Johnson, P.; Chen, W.; Wong, M. W.; Andres, J. L.; Head-Gordon, M.; Replogle, E. S.; Pople, J. A. *Gaussian 98*, revision A.7; Gaussian Inc.: Pittsburgh, PA, 1998.

(12) *ChemOffice 97*, Cambridge Scientific Computing Inc., 875 Massachusetts Ave., Suite 41, Cambridge, MA 02139.

Table 1. Crystal Data and Structure Refinements for [CuCl(pymtH)(dppp)] (**1**), [CuBr(pymtH)(dppp)] (**2**), and [Cu(μ-I)(dppp)]$_2$ (**3**)

	1	**2**	**3**
chem formula	$C_{31}H_{30}ClCuN_2P_2S$	$C_{31}H_{30}BrCuN_2P_2S$	$C_{54}H_{52}Cu_2I_2P_4$
fw	623.56	668.02	602.86
temp/K	120(2)	120(2)	120(2)
λ(Mo Kα)/Å	0.71073	0.71073	0.71073
cryst syst	triclinic	triclinic	triclinic
space group	$P\bar{1}$	$P\bar{1}$	$P\bar{1}$
a/Å	9.86140(10)	9.9021(2)	9.9164(2)
b/Å	10.09070 (10)	10.0952 (2)	10.5308 (2)
c/Å	16.1331 (4)	16.2210 (4)	12.7852 (3)
α/deg	76.5270 (5)	76.8225 (7)	74.905 (2)
β/deg	85.3940 (5)	85.0994 (7)	74.826 (2)
γ/deg	67.3400 (6)	67.3809 (8)	82.5563 (10)
V/Å^3	1440.61 (4)	1457.37 (5)	1246.73 (5)
Z	2	2	2
ρ_{calcd}/g cm^{-3}	1.438	1.522	1.606
μ/mm^{-1}	1.059	2.326	2.255
GOF on F^2 (S)	0.979	1.023	0.958
R [(I > 2σ(I)]	R1 = 0.0325, wR2 = 0.0834	R1 = 0.0365, wR2 = 0.0955	R1 = 0.0299, wR2 = 0.0730
R (all data)	R1 = 0.0421, wR2 = 0.0881	R1 = 0.0442, wR2 = 0.1015	R1 = 0.0365, wR2 = 0.0763
final weighting scheme	*a*	*b*	*c*

[a] Calcd $w = 1/[\sigma^2(F_o^2) + (0.0496P)^2 + 0.6789P]$, where $P = (F_o^2 + 2F_c^2)/3$. [b] Calcd $w = 1/[\sigma^2(F_o^2) + (0.0643P)^2 + 0.6153P]$, where $P = (F_o^2 + 2F_c^2)/3$. [c] Calcd $w = 1/[\sigma^2(F_o^2) + (0.0468P)^2 + 0.1589P]$, where $P = (F_o^2 + 2F_c^2)/3$.

X-ray Crystallographic Study. X-ray diffraction data were collected on an Enraf-Nonius Kappa CCD area-detector diffractometer. The programs DENZO[13] and COLLECT[14] were used in data collection and cell refinement. Details of crystal and structure refinement are shown in Table 1. The structure was solved using program SIR97[15] and refined with program SHELX-97.[16] Molecular plots were obtained with the program ORTEP-3.[17]

Crystallographic data (excluding structure factors) for the structures reported in this paper have been deposited with the Cambridge Crystallographic Data Centre as supplementary publications CCDC-183206 (**1**), CCDC-183207 (**2**), and CCDC-183208 (**3**). Copies of the data can be obtained free of charge on application to CCDC, 12 Union Road, Cambridge CB2 1EZ, U.K. [Fax, international code + 44(1223)336−033; e-mail, deposit@ccdc.cam.ac.uk].

Synthesis of the Complexes. The complexes were prepared according to the following general procedure. A suspension of copper(I) halide (0.5 mmol) and 1,3-propanebis(diphenylphosphine) (206 mg, 0.5 mmol) in 20 cm^3 of acetonitrile was stirred until a white precipitation was formed. A solution of the appropriate thione (0.5 mmol) in methanol was then added, and the new suspension was stirred to clearness. The resulting solution was filtered off, and the clear solution was kept at room temperature. Slow evaporation of the solvent at room temperature gave the microcrystalline solid, which was filtered off and dried in vacuo.

[CuCl(dppp)(pymtH)] (1): orange crystals (255 mg 82%), mp 218−219 °C. Anal. Calcd for $C_{31}H_{30}ClCuN_2P_2S$: C, 59.71; H, 4.85; N, 4.49. Found: C, 59.62; H, 4.76; N, 4.57. IR (cm^{-1}): 3055w, 2887w, 1600vs, 1576vs, 1486vs, 1325vs, 1217s, 1175vs, 1091s, 950vs, 822s, 744vs, 696vs, 505vs, 487vs, 469s. UV−vis (λ_{max}, log ϵ) ($CHCl_3$): 247.5 (4.11), 295.5 (4.24), 408.5 (3.22). ^{1}H NMR ($CDCl_3$, δ ppm): 14.85 (br, 1H, NH_{pymtH}), 7.57 (m, 10H, C_6H_5), 7.24 (m, 12H, C_6H_5 + CH_{pymtH}), 6.51 (t, 1H, CH_{pymtH}), 1.25−2.54 (mm, 6H, dppp).

[CuBr(dppp)(pymtH)] (2): red crystals (280 mg, 84%), mp 215−216 °C. Anal. Calcd for $C_{31}H_{30}BrCuN_2P_2S$: C, 55.74; H, 4.49; N, 4.19. Found: C, 55.94; H, 4.62; N, 2.49. IR (cm^{-1}): 3055m, 2851m, 1600vs, 1564vs, 1480vs, 1427vs, 1324vs, 1205s, 1175vs, 1097s, 971s, 739vs, 696vs, 501vs, 490vs, 475vs. UV−vis (λ_{max}, log ϵ) ($CHCl_3$): 246 (4.16), 295,5 (4.11), 411.5 (2.47). ^{1}H NMR ($CDCl_3$, δ ppm): 14.30 (br, 1H, NH_{pymtH}), 7.56 (m, 10H, C_6H_5), 7.24 (m, 12H, C_6H_5 + CH_{pymtH}), 6.52 (t, 1H, CH_{pymtH}), 1.26−2.54 (mm, 6H, dppp).

[Cu(μ-I)(dppp)]$_2$ (3): colorless crystals (256 mg, 85%), mp 238 °C. Anal. Calcd for $C_{54}H_{52}Cu_2I_2P_4$: C, 53.79; H, 4.31. Found: C, 53.75; H, 4.18. IR (cm^{-1}): 3048m, 2920m, 1582s, 1482vs, 1434vs, 1309s, 1185s, 1098vs, 1026s, 964s, 742vs, 694vs, 509vs, 488vs. UV−vis (λ_{max}, log ϵ) ($CHCl_3$): 245.0 (3.96), 282 (3.68). ^{1}H NMR ($CDCl_3$, δ ppm): 7.47 + 7.23 (mm, 20H, C_6H_5), 1.26−2.44 (mm, 6H, dppp).

[CuCl(dppp)(py2SH)] (4): yellow crystals (271 mg, 87%), mp 170−171 °C. Anal. Calcd for $C_{32}H_{31}ClCuNP_2S$: C, 61.74; H, 4.98; N, 2.25. Found: C, 61.80; H, 4.83; N, 2.22. IR (cm^{-1}): 3042w, 2935m, 1618s, 1582vs, 1480s, 1426vs, 1366vs, 1181s, 1133vs, 1097vs, 1001s, 822vs, 744vs, 696vs, 642s, 511vs, 481vs. UV−vis (λ_{max}, log ϵ) ($CHCl_3$): 249.5 (4.18), 294 (4.26), 393.5 (4.16);). ^{1}H NMR ($CDCl_3$, δ ppm): 14.65 (br, 1H, NH_{py2SH}), 7.56 (m, 10H, C_6H_5), 7.40 (d, 1H, CH_{py2SH}), 7.23 (m, 12H, C_6H_5 + CH_{py2SH}), 6.55 (t, 1H, CH_{py2SH}), 1.71−2.49 (mm, 6H, dppp).

[CuBr(dppp)(py2SH)] (5): yellow crystals (293 mg, 88%), mp 219−220 °C. Anal. Calcd for $C_{32}H_{31}BrCuNP_2S$: C, 57.62; H, 4.65; N, 2.10. Found: C, 56.92; H, 4.93; N, 2.25. IR (cm^{-1}): 3052w, 293om, 1606vs, 1570s, 1488s, 1424vs, 1366s, 1181s, 1133vs,-1097vs, 996vs 750vs, 697vs, 642s, 515vs, 481vs. UV−vis (λ_{max}, log ϵ) ($CHCl_3$): 247 (4.11), 294 (2.15), 391.5 (3.64). ^{1}H NMR ($CDCl_3$, δ ppm): 14.05 (br, 1H, NH_{py2SH}), 7.56 (m, 10H, C_6H_5), 7.46 (d, 1H, CH_{py2SH}), 7.23 (m, 12H, C_6H_5 + CH_{py2SH}), 6.61 (t, 1H, CH_{py2SH}), 1.69−2.54 (mm, 6H, dppp).

[CuCl(dppp)(mtdztH)] (6): yellow crystals (264 mg, 82%), mp 216−217 °C. Anal. Calcd for $C_{30}H_{30}ClCuN_2P_2S_2$: C, 55.98; H, 4.66; N, 2.25. Found: C, 56.19; H, 4.75; N, 2.46. IR (cm^{-1}): 3042w, 1635m, 1570m, 1480s, 1432vs, 1271s, 1161s, 1049s, 738vs, 697vs, 603s, 511vs, 481s. UV−vis (λ_{max}, log ϵ) ($CHCl_3$): 245 (4.09), 386 (4.24). ^{1}H NMR ($CDCl_3$, δ ppm): 14.20 (br, 1H, NH_{mtdztH}), 7.26−7.69 (m, 20H, C_6H_5), 2.42 (s, 3H, CH_3−C), 1.57−2.48 (mm, 6H, dppp).

[CuBr(dppp)(mtdztH)] (7): yellow crystals (162 mg, 47%), mp 218 °C. Anal. Calcd for $C_{30}H_{30}BrCuN_2P_2S_2$: C, 52.35; H, 4.36; N, 4.07. Found: C, 52.07; H, 4.23; N, 3.97. IR (cm^{-1}): 3048w, 2855m, 1618m, 1570m, 1482s, 1459s, 1433vs, 1278s, 1157s, 1097s, 1053s 741vs, 694vs, 511vs, 480s. UV−vis (λ_{max}, log ϵ) ($CHCl_3$): 245 (4.11), 307 (4.09). ^{1}H NMR ($CDCl_3$, δ ppm): 14.20 (br, 1H, NH_{mtdztH}), 7.10−7.56 (m, 20H, C_6H_5), 2.40 (s, 3H, CH_3−C), 2.43−1.57 (mm, 6H, dppp).

[CuCl(dppp)(mftztH)] (8): white crystals (191 mg, 55%), mp 170−171 °C. Anal. Calcd for $C_{31}H_{30}ClCuF_3N_3P_2S$: C, 53.60; H, 4.32; N, 6.08. Found: C, 53.69; H, 4.47; N, 6.11. IR (cm^{-1}): 3055m, 2900m, 1636m, 1588s, 1480vs, 1432vs, 1283vs, 1199vs, 1151vs, 1091vs, 822s, 744vs, 690vs, 547vs, 511vs, 487vs. UV−vis (λ_{max}, log ϵ) ($CHCl_3$): 248 (4.30), 295 (3.88). ^{1}H NMR ($CDCl_3$,

(13) Otwinowski, Z.; Minor, W. In *Macromolecular Crystallography*; Carter, C. W., Jr, Sweet, R. M., Eds.; Methods in Enzymology, Vol. 276; Academic Press: New York, 1997; Part A, pp 307−326.
(14) Hooft, R. *COLLECT Data collection software*; Nonius B.V.: Delft, The Netherlands, 1998.
(15) Altomare, A.; Burla, M. C.; Camalli, M.; Cascarano, G. L.; Giacovazzo, C.; Guagliardi A.; Moliterni, A. G. G.; Polidori, G.; Spagna, R. *J. Appl. Crystallogr.* **1994**, *27*, 435−436.
(16) Sheldrick, G. M.; *SHELXL-97. Program for crystal structure analysis*, release 97-2; University of Göttingen: Göttingen, Germany, 1997.
(17) Farrugia, L. J. *J. Appl. Crystallogr.* **1997**, 30, 565.

δ ppm): 12.02 (br, 1H, NH_{mftztH}), 6.93−7.73 (m, 20H, C_6H_5), 3.54 (s, 3H, CH_3−N), 2.62−1.71 (mm, 6H, dppp).

[CuBr(dppp)(mftztH)] (9): white crystals (196 mg, 53%), mp 231 °C. Anal. Calcd for $C_{31}H_{30}BrCuF_3N_3P_2S$: C, 50.37; H, 4.06; N, 5.68. Found: C, 50.23; H, 4.60; N, 6.20. IR (cm^{-1}): 3055w, 2899w, 1618m, 1584m, 1480vs, 1432vs, 1157vs, 1270s, 1187s, 1097vs 822s, 738vs, 690vs, 505vs, 503vs, 585s. UV−vis (λ_{max}, log ϵ) ($CHCl_3$): 246 (4.13), 292.5 (3.70). ^1H NMR ($CDCl_3$, δ ppm): 7.05−7.74 (m, 20H, C_6H_5), 3.46 (s, 3H, CH_3N), 1.65−2.78 (mm, 6H, dppp).

[CuCl(dppp)(pu6SH)] (10): pale yellow crystals (206 mg, 62%), mp 185−186 °C. Anal. Calcd for $C_{32}H_{30}ClCuN_4P_2S$: C, 56.38; H, 4.69; N, 8.22. Found: C, 64.56; H, 5.34; N, 7.65. IR (cm^{-1}): 3042m, 2899w, 1612s, 1582s, 1493vs, 1474s, 1426s, 1408s, 1181s, 1097vs, 822s, 744vs, 697vs, 643s, 511vs, 481s. UV−vis (λ_{max}, log ϵ) ($CHCl_3$): 245 (3.98), 283.5 (3.92), 396 (2.20). ^1H NMR ($CDCl_3$, δ ppm): 7.06−7.68 (m, 22H, C_6H_5 + CH_{pur6SH}), 1.60−2.55 (mm, 6H, dppp).

[CuBr(dppp)(pu6SH)] (11): orange crystals (290 mg, 82%), mp 226−227 °C. Anal. Calcd for $C_{32}H_{30}BrCuN_4P_2S$: C, 52.92; H, 4.41; N, 7.72. Found: C, 52.89; H, 4.38; N, 7.83. IR (cm^{-1}): 3055m, 2910w, 1612vs, 1540vs, 1480s, 1432vs, 1397vs, 1205s, 1094s, 822s, 738vs, 691vs, 649s, 505vs, 475s. UV−vis (λ_{max}, log ϵ) ($CHCl_3$): 245 (4.07), 284.5 (3.99), 397.5 (2.30). ^1H NMR ($CDCl_3$, δ ppm): 7.08−7.75 (m, 22H, C_6H_5 + CH_{pur6SH}), 1.66−2.52 (mm, 6H, dppp).

[CuCl(dppp)(bzoxtH)] (12): white crystals (295 mg, 89%), mp 159−160 °C. Anal. Calcd for $C_{34}H_{31}ClCuNP_2OS$: C, 61.63; H, 4.45; N, 2.11. Found: C, 59.30; H, 5.68; N, 2.19. IR (cm^{-1}): 3052w, 2886w, 1612m, 1588m, 1504vs, 1438s, 1253vs, 1187s, 1139vs, 1097vs, 929s, 816s, 738vs, 697vs, 511vs, 481s. UV−vis (λ_{max}, log ϵ) ($CHCl_3$): 255 (4.14), 298.5 (4.39). ^1H NMR ($CDCl_3$, δ ppm): 13.30 (br, 1H, NH_{bzoxtH}), 7.20−7.72 (m, 24H, C_6H_5 + CH_{bzoxtH}), 1.78−2.47 (mm, 6H, dppp).

[CuBr(dppp)(bzoxtH)] (13): white crystals (180 mg (51%), mp 218 °C. Anal. Calcd for $C_{34}H_{31}BrCuNP_2OS$: C, 57.74; H, 4.38; N, 1.98. Found: C, 58.32; H, 4.64; N, 1.97. IR (cm^{-1}): 3054w, 2887w, 1612s, 1584m, 1504m, 1480vs, 1432vs, 1270s, 1187s, 1097vs, 1139vs, 1097vs, 959s, 822s, 744vs, 690vs, 505vs, 480s. UV−vis (λ_{max}, log ϵ) ($CHCl_3$): 245 (4.11), 285.0 (3.65). ^1H NMR ($CDCl_3$, δ ppm): 13.25 (br, 1H, NH_{bzoxtH}), 7.20−7.73 (m, 24H, C_6H_5 + CH_{bzoxtH}), 1.56−2.47 (mm, 6H, dppp).

[CuCl(dppp)(mbzimtH)] (14): pale yellow crystals (304 mg, 90%), mp 159−160 °C. Anal. Calcd for $C_{35}H_{34}ClCuN_2P_2S$: C, 62.22; H, 5.03; N, 4.34. Found: C, 63.05; H, 5.12; N, 4.42. IR (cm^{-1}): 3055w, 2885w, 1612s, 1588m, 1480vs,1432vs, 1378s, 1324s, 1175vs, 1097vs, 966s, 798s, 744vs, 697vs, 630s, 547vs, 505vs, 481s. UV−vis (λ_{max}, log ϵ) ($CHCl_3$): 250 (4.23), 303 (4.38). ^1H NMR ($CDCl_3$, δ ppm): 11.71 (br, 2H, $NH_{mbzimtH}$), 6.85−7.72 (m, 23H, C_6H_5 + $CH_{mbzimtH}$), 2.24 (s, 3H, CH_3−C_{Ph}), 1.71−2.71 (mm, 6H, dppp).

[CuBr(dppp)(mbzimtH)] (15): pale yellow crystals (331 mg, 92%), mp 218 °C. Anal. Calcd for $C_{35}H_{34}BrCuN_2P_2S$: C, 57.62; H, 4.65; N, 2.25. Found: C, 56.02; H, 4.93; N, 2.10. IR (cm^{-1}): 3052w, 2882w, 1612vs, 1586s, 1514vs, 1464vs, 1325vs, 1181vs, 1097vs, 966s, 800vs, 738vs, 696vs, 629s, 544s, 510vs, 482vs. UV−vis (λ_{max}, log ϵ) ($CHCl_3$): 246 (4.04), 313.5 (4.20). ^1H NMR ($CDCl_3$, δ ppm): 11.95 (br, 2H, $NH_{mbzimtH}$), 6.80−7.71 (m, 23H, C_6H_5 + $CH_{mbzimtH}$), 2.25 (s, 3H, CH_3−C_{Ph}), 1.71−2.59 (mm, 6H, dppp).

Results and Discussion

Synthesis. Diphosphines have been frequently used for bridging or chelation of two low oxidation state transition metal centers. Among the acyclic diphosphines of the type $Ph_2P(CH_2)_nPPh_2$, we have expected 1,2-ethanebis(diphenylphosphine) (dppe) to be the best canditate for chelating copper(I). However, dppe appears to act as a bridging rather than as a chelating ligand, as it was demonstrated at least in the case of copper(I) bromide.[6] Contrary to this previous observation we succeeded in chelating Cu(I) using the larger 1,3-propanebis(diphenylphosphine) (dppp). It should be noted that only a few copper(I) complexes containing dppp as a chelating ligand have been structurally characterized so far, most of them being polynuclear aggregates, but also two examples of mononuclear cations of the type $[Cu(dppp)_2]^+$.

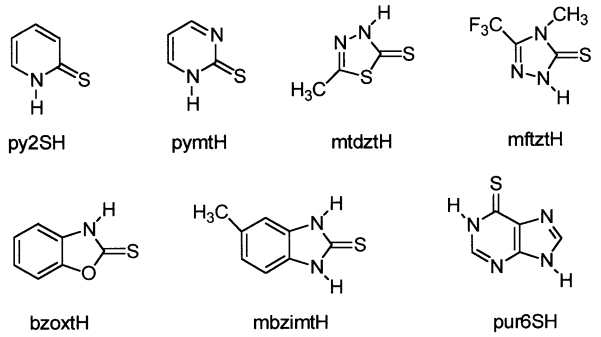

Figure 1. The heterocyclic thione ligands used with their abbreviations.

Treatment of equimolar quantities of copper(I) chloride or copper(I) bromide and 1,3-propanebis(diphenylphosphine) (dppp) followed by the addition of 1 equiv of the appropriate thione (L) [L = pyridine-2-thione (py2SH), pyrimidine-2-thione (pymtH), 5-methyl-1,3,4-thiazole-2-thione (mtdztH), 4-methyl-5-trifluoromethyl-4*H*-1,2,4-triazoline-3(2*H*)-thione (mftztH), 6-mercaptopurine (pur6SH), benz-1,3-oxazole-2-thione (bzoxtH), 5-methylbenz-1,3-imidazole-2-thione (mbzimtH) (Figure 1)] in dry acetonitrile/methanol solution yields monomeric mixed ligand complexes of the type [CuX(dppp)L] with the neutral heterocyclic thiones acting in an S-monodentate coordination mode, despite their potentially ambidentate character. On the contrary, reaction of copper(I) iodide under the same conditions proceeds in a different way to give the dimeric complex $[Cu(\mu\text{-}I)(dppp)]_2$. Single crystals of **1**−**3** suitable for X-ray analysis are obtained from the initial products deposited from the reactions by slow evaporation of their acetonitrile solutions. Compounds **1**−**15** are microcrystalline solids slightly soluble in chloroform, methanol, ethanol, and acetone and moderately soluble in acetonitrile. They are stable to air and moisture and can be manipulated in air without appreciable decomposition. The composition of the compounds has been confirmed by elemental analysis. Their solutions in acetone and chloroform are nonconducting. Room temperature magnetic measurements confirm the diamagnetic nature of the compounds.

Spectroscopy. The electronic absorption spectra of the complexes in chloroform solutions appear to be mainly of intraligand character, presenting two broad bands with maxima in the 245−255 and 280−310 nm regions, respectively. The first one can be attributed to intraligand $\pi^* \leftarrow \pi$ transitions on the phenyl groups of the phosphine ligand, since the uncoordinated 1,3-propanebis(diphenylphosphine) reveals a strong absorption at 253.5 nm which usually remain

Table 2. Selected Bond Distances (Å) and Bond Angles (deg) for [CuCl(pymtH)(dppp)] (**1**)

Cu(1)−P(1)	2.2698(5)	P(1)−C(26)	1.8348(19)
Cu(1)−P(2)	2.2701(5)	P(1)−C(19)	1.8487(18)
Cu(1)−S(1)	2.2924(5)	P(2)−C(5)	1.8253(19)
Cu(1)−Cl(1)	2.4071(5)	P(2)−C(11)	1.8314(19)
S(1)−C(1)	1.6946(19)	P(2)−C(17)	1.8432(19)
P(1)−C(20)	1.8208(19)		
P(1)−Cu(1)−P(2)	99.649(19)	C(26)−P(1)−Cu(1)	122.75(6)
P(1)−Cu(1)−S(1)	124.393(19)	C(19)−P(1)−Cu(1)	107.75(6)
P(2)−Cu(1)−S(1)	114.891(19)	C(5)−P(2)−C(11)	104.55(8)
P(1)−Cu(1)−Cl(1)	103.256(18)	C(5)−P(2)−C(17)	104.68(9)
P(2)−Cu(1)−Cl(1)	98.526(18)	C(11)−P(2)−Cu(11)	101.46(8)
S(1)−Cu(1)−Cl(1)	112.387(18)	C(5)−P(2)−C(1)	116.94(6)
C(1)−S(1)−Cu(1)	112.35(6)	C(11)−P(2)−C(1)	119.81(6)
C(20)−P(1)−C(26)	102.55(8)	C(17)−P(2)−Cu(1)	107.37(6)
C(20)−P(1)−C(19)	105.68(9)	C(18)−C(17)−P(2)	113.61(13)
C(26)−P(1)−C(19)	99.25(8)	C(17)−C(18)−C(19)	116.20(16)
C(20)−P(1)−Cu(1)	116.50(6)	C(18)−C(19)−P(1)	117.79(13)

unshifted upon coordination to Cu(I). The lower energy band lies in the region where the free thiones absorb, expressing a small red shift as a consequence of the coordination to Cu(I) and should be, therefore, considered as a thione-originating intraligand transition which possess some MLCT character.[18,19] The infrared spectra of compounds **1**−**15**, recorded in the range 4000−250 cm^{-1}, show all the expected strong phosphine bands, which remain practically unshifted upon coordination. Moreover, with the exception of the spectrum of the iodo compound (**3**), they contain all of the bands due to the presence of the heterocyclic thione ligands. In detail, they exhibit the usual four "thioamide bands" in the regions ∼1510, 1320, 1000, and 750 cm^{-1}, although in some cases partly masked by strong phosphine absorptions, as well as the characteristic NH stretching vibrations observed in the ∼3150 cm^{-1} region. The shifts observed for these bands due to coordination in conjunction with the lack of ν(SH) bands at ca. 2500−2600 cm^{-1} signify the exclusive S-coordination mode of the thione ligands. Room temperature ^{1}H NMR spectra recorded in deuterated chloroform display, apart from the signals expected for the phosphine and thione ligands, a single broad resonance at ∼14 ppm attributed to the NH proton reflecting the prevalence of the thione tautomer in the complexes.

Description of the Structures. [CuCl(dppp)(pymtH)] (1) and [CuBr(dppp)(pymtH)] (2). Selected bond lengths and angles for compounds **1** and **2** are given in Tables 2 and 3, and perspective drawings showing the atom numbering are shown in Figures 2 and 3, respectively. In both complexes copper(I) exhibits a highly distorted tetrahedral coordination geometry, with the metal atom being surrounded by two P, one S, and one halide donor atoms. The largest deviation from the ideal geometry is reflected on the P(1)−Cu(1)−S(1) bond angles whose values (124.393(19)° in **1** and 125.52(2)° in **2**, respectively) are markedly higher than the tetrahedral value of 109.4°. It is interesting to note that, for a series of monomeric copper(I) halide complexes involving one heterocyclic thione and two monodentate triphenylphosphine ligands, exhibiting the same $CuSP_2X$ core,[3,5] the largest angle was found, as expected, between the two most bulky phosphine ligands. In the two complexes under investigation, however, the chelating dppp ligand is coordinated to the copper(I) center with a P−Cu−P angle of 99.649(19)° for **1** and 99.59(2)° for **2**, which is well below what is ideal for a tetrahedrally coordinated metal ion. The strong intramolecular

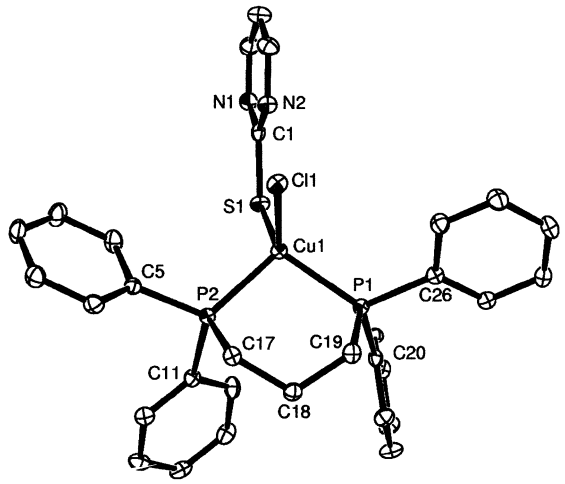

Figure 2. Thermal ellipsoid drawing of the crystal structure of **1** at the 50% probability level with the labeling scheme.

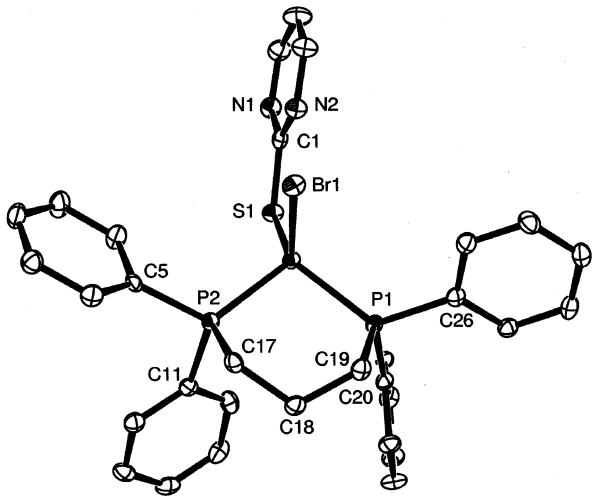

Figure 3. Thermal ellipsoid drawing of the crystal structure of **2** at the 50% probability level with the labeling scheme.

Table 3. Selected Bond Distances (Å) and Bond Angles (deg) for [CuBr(pymtH)(dppp)] (**2**)

Cu(1)−P(1)	2.2688(6)	P(1)−C(26)	1.835(3)
Cu(1)−P(2)	2.2715(7)	P(1)−C(19)	1.849(2)
Cu(1)−S(1)	2.2903(6)	P(2)−C(5)	1.826(2)
Cu(1)−Br(1)	2.5369(4)	P(2)−C(11)	1.834(2)
S(1)−C(1)	1.690(3)	P(2)−C(17)	1.838(2)
P(1)−C(20)	1.820(2)		
P(1)−Cu(1)−P(2)	99.59(2)	C(26)−P(1)−Cu(1)	123.53(8)
P(1)−Cu(1)−S(1)	125.52(2)	C(19)−P(1)−Cu(1)	107.77(8)
P(2)−Cu(1)−S(1)	114.65(2)	C(5)−P(2)−C(11)	104.38(11)
P(1)−Cu(1)−Br(1)	102.553(19)	C(5)−P(2)−C(17)	104.62(11)
P(2)−Cu(1)−Br(1)	96.775(19)	C(11)−P(2)−C(17)	101.31(11)
S(1)−Cu(1)−Br(1)	113.245(19)	C(5)−P(2)−Cu(1)	116.71(8)
C(1)−S(1)−Cu(1)	113.13(9)	C(11)−P(2)−Cu(1)	119.99(8)
C(20)−P(1)−C(26)	102.61(11)	C(17)−P(2)−Cu(1)	107.80(8)
C(20)−P(1)−C(19)	105.62(11)	C(18)−C(17)−P(2)	113.71(16)
C(26)−P(1)−C(19)	99.28(11)	C(17)−C(18)−C(19)	115.9(2)
C(20)−P(1)−Cu(1)	115.69(8)	C(18)−C(19)−P(1)	118.26(16)

(18) Del Paggio, A. A.; McMillin, D. R. *Inorg. Chem.* **1983**, *22*, 691−692.
(19) Kutal, C. *Coord. Chem. Rev.* **1990**, *90*, 213−253.

Table 4. Selected Bond Distances (Å) and Bond Angles (deg) for $[Cu(\mu\text{-}I)(dppp)]_2$ (**3**)

Cu(1)−I(1)	2.6470(3)	P(1)−C(13)	1.846(2)
Cu(1)#1−I(1)[a]	2.6823(3)	P(2)−C(16)	1.832(3)
Cu(1)−P(1)	2.2658(7)	P(2)−C(22)	1.831(3)
Cu(1)−P(2)	2.2704(7)	P(2)−C(15)	1.841(3)
Cu(1)−I(1)#(1)	2.6823(3)	C(13)−C(14)	1.537(4)
P(1)−C(1)	1.836(3)	C(14)−C(15)	1.542(4)
P(1)−C(7)	1.822(3)		

Cu(1)−I(1)−Cu(1)#1	77.231(11)	C(1)−P(1)−Cu(1)	125.14(9)
P(1)−Cu(1)−P(2)	102.73(2)	C(13)−P(1)−Cu(1)	107.17(9)
P(1)−Cu(1)−I(1)	124.63(2)	C(22)−P(2)−C(16)	103.64(11)
P(2)−Cu(1)−I(1)	112.42(2)	C(22)−P(2)−C(15)	103.13(12)
P(1)−Cu(1)−I(1)#1	110.94(2)	C(16)−P(2)−Cu(15)	103.00(12)
P(2)−Cu(1)−I(1)#1	101.13(2)	C(22)−P(2)−Cu(1)	118.40(8)
I(1)−Cu(1)−I(1)#1	102.769(10)	C(16)−P(2)−Cu(1)	118.92(8)
C(7)−P(1)−C(1)	102.35(12)	C(15)−P(2)−Cu(1)	107.66(9)
C(7)−P(1)−C(13)	103.95(12)	C(14)−C(13)−P(1)	116.23(17)
C(1)−P(1)−C(13)	98.59(11)	C(13)−C(14)−C(15)	115.1(2)
C(7)−P(1)−Cu(1)	116.50(8)	C(14)−C(16)−P(2)	114.62(17)

[a] # indicates coordinates transposed by $1 - x, -y, 2 - z$.

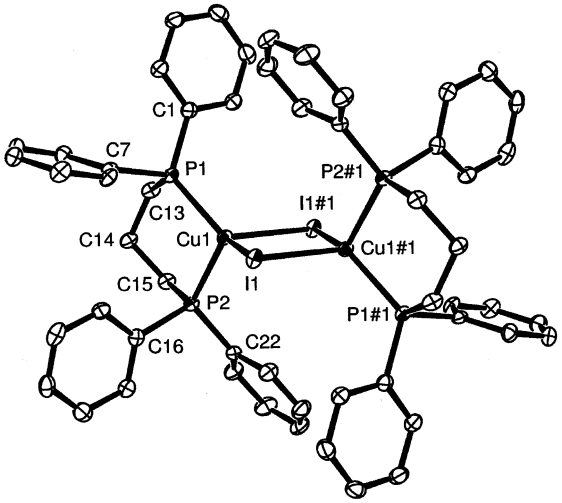

Figure 4. Thermal ellipsoid drawing of the crystal structure of **3** at the 50% probability level with the labeling scheme.

hydrogen bond between the halogen and the N(1)H can hardly be responsible for these rather large distortions since the same bite angle for the six-membered ring was also found in $[Cu(dppp)_2]BF_4$.[20] The two individual Cu−P distances are somewhat shorter than those found in $[Cu(dppp)_2]BF_4$ or in other monomeric copper(I) complexes with chelating diphosphines, e.g., in $[Cu(dppe)_2]ClO_4$. Finally, the Cu−S, Cu−Cl, and Cu−Br bond lengths lie in the range normally observed for tetrahedrally coordinated copper(I) complexes with terminal chlorine, bromine, and thione-sulfur donors.

$[Cu(\mu\text{-}I)(dppp)]_2$ (3). Selected interatomic distances and angles are given in Table 4. This complex consists of discrete centrosymmetric dimers in which the two copper atoms are doubly bridged by the iodide ligands to form a four-membered Cu_2I_2 ring with a Cu···Cu separation of 3.3261(6) Å (Figure 4). The strongly distorted tetrahedral coordination around each copper(I) central atom is completed by the two P donor atoms of the chelating dppp ligand. It should be noted that copper(I) iodide usually tends to form dimeric complexes with two iodine atoms serving as bridges between the two copper atoms, although there are also some representatives of mononuclear species with a $CuIP_2S$ core among the structures characterized by us so far.[3f,21] This is not unexpected for a typically soft acceptor such as the monovalent copper which strongly prefers soft ligands such as iodide. It is remarkable that the strong tendency of copper(I) to bind iodide ligands together with the formation of stable six-membered chelate rings results in an exclusion of the thione ligand from the coordination sphere. The same holds also true for the 1,5-pentanebis(diphenylphosphine) (dpppe) ligand, which also reacts with copper(I) iodide to give the dimeric $[Cu(\mu\text{-}I)(dpppe)]_2$, even in the presence of 1 equiv of a heterocyclic thione ligand.[22] In contrast in the dppp complex, each of the two diphosphine ligands of the dpppe molecule does not chelate at a single copper center but bridges intramolecularly the two metal centers, probably because of the much weaker stabilizing effect of the eight-membered ring. Considering the geometrical parameters of the dppp ligand one would expect only minor differences between the two monomeric complexes **1** and **2** and the dimeric complex **3**. The six-membered chelate ring in all three complexes has the expected chair conformation, while the distances of the two individual Cu−P bonds are almost equal in the three complexes and show a small asymmetry of the same magnitude, with the bite angle of the phosphine ligand in **3** being enlarged only by ca. 3° when compared with that in **1** and **2**. Within the Cu_2I_2 backbone, the two Cu−I bond distances of 2.6470(3) and 2.6823(3) Å are clearly longer than those found for tetrahedral Cu(I) in monomeric complexes but only slightly shorter than the corresponding bond distances observed in bis[μ-iodo(pyridine-2-thione)(tri-*m*-tolylphosphine)copper(I)].[4b] Moreover, there is a quite large asymmetry in the Cu_2I_2 core of **3** with regard to these bond distances, much larger than in the above menthioned mixed-ligand dimer. Surprisingly, the I−Cu−I and Cu−I−Cu angles, 77.23° and 102.77°, respectively, are far from the predicted geometry for $Y_2MX_2MY_2$ dimers assumed by Summerville and Hoffmann for d^{10} systems (Cu−I−Cu = 94°), but also disagree with the ideal values (109.5° and 70.5°) calculated for a symmetric dimer.[23]

Computational Studies Using DFT. Equilibrium Geometry, Electronic Structure, and Bonding Mechanism in Mononuclear $[CuX(PH_3)_2]$ and [CuX(1,3-pdp)] (X = Cl, Br, or I) Compounds. Let us first explore the details of the structural, energetic, and electronic properties of the mononuclear $[CuX(PH_3)_2]$ and [CuX(1,3-pdp)] compounds (X = Cl, Br, I; 1,3-pdp = 1,3-propylene-diphosphine ligand formulated as $H_2PCH_2CH_2CH_2PH_2$). Selected geometrical parameters of the $[CuX(PH_3)_2]$ and [CuX(1,3-pdp)] complexes along with their total electronic energies, dipole moments, and some electronic properties are given in Tables 5 and 6, respectively. The $[CuX(PH_3)_2]$ and [CuX(1,3-pdp)]

(20) Comba, P.; Katsichtis, C.; Nuber B.; Pritzkow, H. *Eur. J. Inorg. Chem.* **1999**, 777−788.

(21) Aslanidis, P.; Cox, P. J.; Karagiannidis, P.; Hadjikakou, S. K.; Antoniadis, C. D. *Eur. J. Inorg. Chem.* **2002**, 2216−2222.

(22) Kokkou, S. C.; Voutsas, G.; Aslanidis, P.; Karagiannidis, P. Submitted to *Acta Crystallogr.*

(23) Summerville, R. H.; Hoffmann, R. *J. Am. Chem. Soc.* **1976**, *98*, 7240−7254.

Table 5. Selected Structural Parameters, Total Energies, and Electronic Properties of $CuX(PH_3)_2$ (X = Cl, Br, I) Compounds Computed at the B3LYP/SDD Level of Theory

	$CuCl(PH_3)_2$	$CuBr(PH_3)_2$	$CuI(PH_3)_2$
E (hartrees)	−1343.79263	−896.99300	−895.03252
R_e(Cu−X) (Å)	2.240	2.364	2.532
R_e(Cu−P) (Å)	2.324	2.328	2.339
θ_e(P−Cu−X) (deg)		113.2113.3	113.9
θ_e(P−Cu−P) (deg)		133.5133.4	132.2
μ_e (D)	7.30	7.95	8.09
η (eV)	2.362	2.329	2.213
q_{Cu}[a]	0.56 (0.19)[b]	0.56 (0.24)	0.51 (0.20)
q_X	−0.73 (−0.36)	−0.75 (−0.44)	−0.70 (−0.40)
q_P	−0.07 (−0.11)	−0.07 (−0.10)	−0.08 (−0.10)
bop(Cu−X)[c]	0.362	0.302	0.314
bop(Cu−P)	0.020	0.042	0.044
nec(Cu)[d]	$4s^{0.49}3d^{9.88}$	$4s^{0.49}3d^{9.90}$	$4s^{0.53}3d^{9.91}$
nec(X)	$4s^{1.97}3d^{5.76}$	$4s^{1.97}3d^{5.78}$	$4s^{1.97}3d^{5.73}$

[a] Natural charges. [b] Figures in parentheses are the Mulliken net atomic charges. [c] Mulliken bond overlap population. [d] Natural electron configuration.

Table 6. Selected Structural Parameters, Total Energies, and Electronic Properties of CuX(1,3-pdp) (X = Cl, Br, I) Compounds Computed at the B3LYP/SDD Level of Theory

	CuCl(1,3-pdp)	CuBr(1,3-pdp)	CuI(1,3-pdp)
E (hartrees)	−1360.44684	−1013.64676	−1010.68645
R_e(Cu−X) (Å)	2.204	2.326	2.496
R_e(Cu−P) (Å)	2.355	2.365	2.366
θ_e(P−Cu−X) (deg)	131.2	131.5	131.3
θ_e(P−Cu−P) (deg)	97.3	96.8	97.1
μ_e (D)	10.77	11.46	11.65
η (eV)	2.195	2.177	2.079
q_{Cu}[a]	0.55(0.05)[b]	0.56 (0.14)	0.51 (0.10)
q_X	−0.70 (−0.38)	−0.73 (−0.46)	−0.68 (−0.43)
q_P	0.15 (0.16)	0.15 (0.15)	0.15 (0.15)
bop(Cu−X)[c]	0.341	0.273	0.275
bop(Cu−P)	0.110	0.110	0.108
nec(Cu)[d]	$4s^{0.51}3d^{9.87}$	$4s^{0.51}3d^{9.89}$	$4s^{0.55}3d^{9.90}$
nec(X)	$4s^{1.96}3d^{5.74}$	$4s^{1.96}3d^{5.76}$	$4s^{1.96}3d^{5.71}$

[a] Natural charges. [b] Figures in parentheses are the Mulliken net atomic charges. [c] Mulliken bond overlap population. [d] Natural electron configuration.

complexes are three-coordinated with a trigonal planar coordination environment shown in Figure 5. In the $[CuX(PH_3)_2]$ complexes the three donor and the copper central atoms are found in a plane. However, in the [CuX(1,3-pdp)] analogues there is a deviation of the copper(I) atom from the plane defined by the three donor atoms amounting to 0.026, 0.026, and 0.019 Å for the chloro, bromo, and iodo derivatives, respectively. The metallacycle chelate ring adopts a chair configuration (Figure 5b) with a ∠P−Cu−P bond angle of about 97° and exhibits a symmetry plane defined by X, Cu, and the central C atom of the bidentate pdp ligand. This bond angle is larger by about 36° in the $[CuX(PH_3)_2]$ complexes involving the unidentate phosphine ligand. It can also be seen that there are no significant structural changes in $[CuX(PH_3)_2]$ and [CuX(1,3-pdp)] complexes due to the influence of the identity of the halide ligand X. Noteworthy is the small elongation of the Cu−P bond in the iodo compound by 0.015 and 0.011 Å with respect to the chloro and bromo analogues, respectively, followed by a concomitant narrowing of the ∠P−Cu−P bond angle by about 1.2°. A small elongation of the Cu−P bond is also observed in the iodo derivative of the [CuX(1,3-pdp)] complexes, but

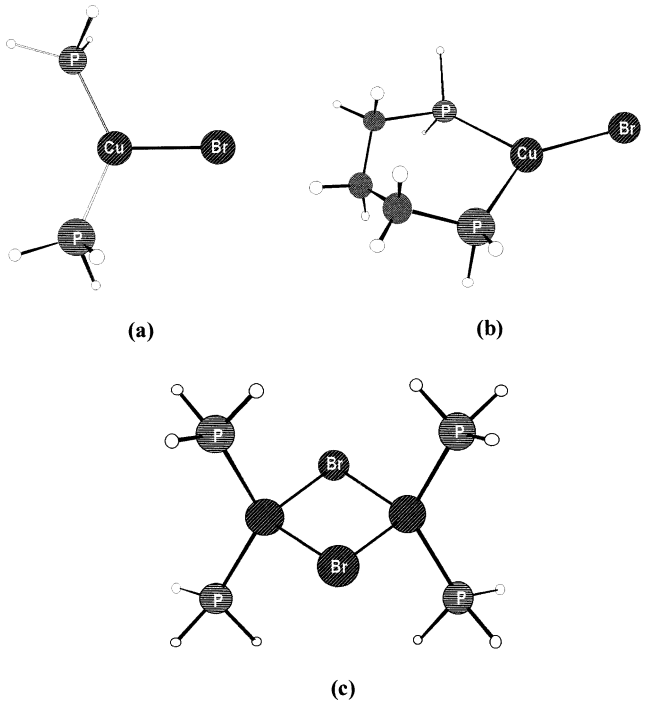

Figure 5. Equilibrium structures of the $CuX(PH_3)_2$ (a), CuX(1,3-pdp) (b), and $[Cu(\mu\text{-}X)(PH_3)_2]_2$ (c) complexes computed at the B3LYP/SDD level of theory.

only with respect to the chloro derivative, the elongation being 0.011 Å. On the other hand, the Cu−X bond lengths are affected by the phosphine ligand. Interestingly, the Cu−Cl, Cu−Br, and Cu−I bonds in $[CuX(PH_3)_2]$ complexes are lengthened by about 0.036 Å compared to the corresponding bonds of the [CuX(1,3-pdp)] complexes. Moreover, the Cu−X bond lengths in both series of complexes following the expected trend Cu−Cl < Cu−Br < Cu−I are in excellent agreement with available experimental data.[24] The experimentally determined Cu−I bond length of 2.591 Å in the analogous $[CuI(PCy_3)_2]$ complex compares well with the computed Cu−I bond length of the $[CuI(PH_3)_2]$ compound.[12a] The observed elongation of the Cu−I bond (by 0.059 Å) in the $[CuI(PCy_3)_2]$ complex is the result of the stronger inductive effect of the PCy_3 than the PH_3 ligand (PCy_3 is a stronger σ donor than PH_3). Noteworthy is the excellent agreement of the computed ∠P−Cu−P bond angle in the $[CuI(PH_3)_2]$ compound (132.2°) and the experimentally determined one in the the $[CuI(PCy_3)_2]$ complex (134.06°) in spite of the bulky PCy_3 ligands. The experimentally determined ∠P−Cu−P bond angles in $[CuI(PPh_3)_2]$ and $[CuI(PPh_2)(o\text{-tolyl})]$ compounds[12b,c] are 126.9° and 126.4°, respectively. The ν(Cu−X) stretching vibrational frequencies appearing at 320 (351) cm^{-1}, 238 (274) cm^{-1}, and 182 (198) cm^{-1}, for the chloro, bromo, and iodo derivatives of the $[CuX(PH_3)_2]$ and [CuX(1,3-pdp)] complexes, respectively, are compatible with the computed Cu−X bond lengths.

(24) (a) Soloveichik, G. L.; Eisenstein, O.; Poulton, J. T.; Streib, W. E.; Huffman, J. C.; Caulton, K. G. *Inorg. Chem.* **1992**, *31*, 3306−3312. (b) Bowmaker, G. A.;. Dyason, J. C.; Healy, P. C.; Engelhardt, L. M.; Pakauatchai, C.; White, A. H. *J. Chem. Soc., Dalton Trans.* **1987**, 1089−1091. (c) Bowmaker, G. A.; Engelhardt, L. M.; Healy, P. C.; Kildea, J. D.; Papasergio, R. I.; White, A. H. *Inorg. Chem.* **1987**, *26*, 3533−3538.

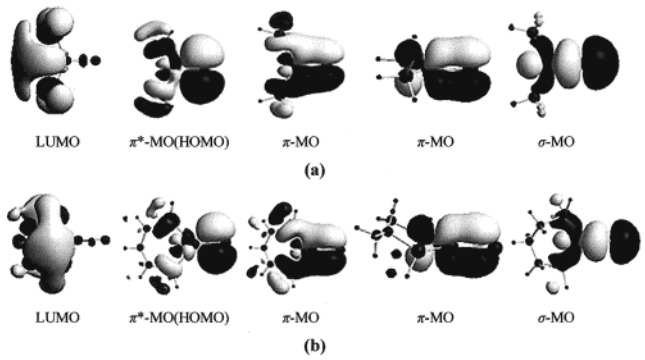

Figure 6. Representative FMOs of the $CuX(PH_3)_2$ (a) and CuX(1,3-pdp) (b) molecules, along with the MOs describing the Cu−X interactions.

Finally, the computed dipole moments of the $[CuX(PH_3)_2]$ and [CuX(1,3-pdp)] complexes illustrate that their polarity follows the order I > Br > Cl.

The population analysis (both Mulliken and natural bond orbital, NBO) indicated that the Cu(I) metal center upon coordination accepts electron density from both the halide and phosphine ligands, thus acquiring a positive natural charge of about 0.5−0.6 charge unit (0.19−0.24 and 0.05−0.14 charge unit from the Mulliken population analysis of the wave functions of the $[CuX(PH_3)_2]$ and [CuX(1,3-pdp)] complexes, respectively). Notice that the natural electron configuration (*nec*) on the Cu central atom and the halide ligands assigned by the NBO analysis is not affected significantly by the nature of the halide and phosphine ligands. Interestingly, the computed bond overlap populations (*bop*) of the Cu−X and Cu−P bonds do not correlate with the computed bond lengths; thereby the metal−ligand interactions in the $[CuX(PH_3)_2]$ and [CuX(1,3-pdp)] complexes should exhibit a strong covalent component. This is substantiated by the respective molecular orbitals (MOs) describing the corresponding coordination bonds. Representative frontier molecular orbitals (FMOs) of the $[CuX(PH_3)_2]$ and [CuX(1,3-pdp)] molecules, along with the MOs describing the Cu−X interactions, are depicted schematically in Figure 6. It can be seen that the Cu−X bond is a composite bond involving both σ and π components, thus acquiring a partially double bond character. The highest occupied MO (HOMO) corresponding to a π^* antibonding Cu−X interaction is strongly polarized toward the halide ligand. On the other hand, the lowest unoccupied MO (LUMO) corresponds to a delocalized MO over the H atoms of the phosphine ligands with a small contribution from a d orbital of the Cu(I) central atom, as well. On the basis of the nature of the FMOs it can be envisaged that all monomers could be dimerized through the favorable HOMO−LUMO interactions. The tendency for dimerization is expected to be greater for the iodo derivative exhibiting the lower HOMO−LUMO energy gap (less hardness) than for the chloro and bromo derivatives in both series of complexes. Compare the hardness values η of the $[CuX(PH_3)_2]$ and [CuX(1,3-pdp)] complexes shown in Tables 5 and 6, respectively. The hardness η was defined by Parr and Pearson[25] as $\eta = {}^1/_2(\mathrm{IP} - \mathrm{EA}) = {}^1/_2(\epsilon_{\mathrm{LUMO}} - \epsilon_{\mathrm{HOMO}})$, where IP and EA are the first vertical ionization potential and electron affinity of the species, which in the framework of Koopman's theorem can be approximated by ϵ_{HOMO} and ϵ_{LUMO} with opposite sign, respectively.

Table 7. Selected Structural Parameters, Total Energies, and Electronic Properties of $[Cu(\mu\text{-}X)(PH_3)_2]_2$ (X = Cl, Br, I) Dimers Computed at the B3LYP/SDD Level of Theory

	$[Cu(\mu\text{-}Cl)(PH_3)_2]_2$	$[Cu(\mu\text{-}Br)(PH_3)_2]_2$	$[Cu(\mu\text{-}I)(PH_3)_2]_2$
E (hartrees)	−1343.85528	−1794.01037	−1790.08777
R_e(Cu−X) (Å)	2.464	2.600 (2.580) 2.570 (2.590)[a]	2.745
R_e(Cu−P) (Å)	2.339	2.345	2.369
R_e(Cu···Cu) (Å)	3.130	3.094	2.895
θ_e(X−Cu−X) (deg)	101.1	106.5	116.4
θ_e(Cu−X−Cu) (deg)	78.9	73.7 (73.3)	63.7
θ_e(P−Cu−P) (deg)	127.0	126.1	122.2
τ(P−P−Cu−X) (deg)	118.5	122.0 (125.2)	126.2 (126.5)
μ_e (D)	0.01	0.06	0.02
η (eV)	2.264	2.213	2.167
q_{Cu}[a]	0.58 (0.28)[c]	0.57 (0.29)	0.49 (0.23)
q_X	−0.72 (−0.35)	−0.73 (−0.40)	−0.64 (−0.35)
q_P	−0.05 (−0.12)	−0.05 (−0.11)	−0.06 (−0.10)
bop(Cu−X)[d]	0.188	0.157	0.159
bop(Cu−P)	−0.072	−0.020	−0.017
bop(Cu···Cu)	−0.367	−0.107	−0.366
nec(Cu)[e]	$4s^{0.46}3d^{9.91}$	$4s^{0.47}3d^{9.91}$	$4s^{0.53}3d^{9.93}$
nec(X)	$4s^{1.96}3d^{5.76}$	$4s^{1.96}3d^{5.76}$	$4s^{1.96}3d^{5.68}$

[a] These four values correspond to four inequivalent Cu−Br bonds. [b] Natural charges. [c] Figures in parentheses are the Mulliken net atomic charges. [d] Mulliken bond overlap population. [e] Natural electron configuration.

Equilibrium Geometry, Electronic Structure, and Bonding Mechanism in Binuclear $[Cu(\mu\text{-}X)(PH_3)_2]_2$ (X = Cl, Br, or I) Model Compounds. To obtain a computationally convenient size for the dinuclear $[Cu(\mu\text{-}X)(1,3\text{-dppp})]_2$ (X = Cl, Br, or I) compounds, we used only model compounds involving the unsubstituted phosphine ligands. The use of such models does not alter significantly the description of the "core" region of the compounds and is ultimately the most efficient and productive route to modeling the electronic structure and related properties of the real large-sized dinuclear $[Cu(\mu\text{-}X)(1,3\text{-dppp})]_2$ complexes. The $[Cu(\mu\text{-}X)(PH_3)_2]_2$ dimers are predicted to be thermodynamically more stable than the monomers, the computed heats $\Delta_R H$ of the dimerization processes being equal to 20.9, 15.3, and 14.3 kcal mol^{-1}, for the chloro, bromo, and iodo derivatives, respectively, at the B3LYP/SDD level of theory. Selected geometrical parameters of the $[Cu(\mu\text{-}X)(PH_3)_2]_2$ dimers along with their total electronic energies, dipole moments and some electronic properties are given in Table 7. The equilibrium geometry of the $[Cu(\mu\text{-}X)(PH_3)_2]_2$ dimers, except of the bromo derivative, exhibiting D_{2h} symmetry, corresponds to a diamond-like structure (Figure 5c) with the Cu−X bond distances defining the $Cu(\mu\text{-}X)_2Cu$ rhombus being equivalent. Surprisingly, in the bromo derivative there are no equivalent Cu−Br bond distances in the $Cu(\mu\text{-}Br)_2Cu$ rhombus, the Cu−Br bond lengths being 2.600, 2.580, 2.590, and 2.570 Å. The Cu−X bond lengths in the dimers are longer by about 0.22 Å relative to the corresponding bonds of the monomers. The intermetallic Cu···Cu distance is tuned by the identity

(25) (a) Parr, R. G.; Pearson, R. G. *J. Am. Chem. Soc.* **1983**, *105*, 7512−7516. (b) Pearson, R. G. *J. Chem. Educ.* **1987**, *64*, 561−565. Pearson, R. G. *Acc. Chem. Res.* **1993**, *26*, 250−255.

of the halide ligand, X, following paradoxically the trend Cu(μ-I)Cu < Cu(μ-Br)Cu < Cu(μ-Cl)Cu. The shortest Cu···Cu distance was observed for the best electron-donating bridged iodide ligand. A similar observation has previously been made by Soloveichik et al.[12a] for the [$L_nCu^I(\mu$-X)Cu^IL_n] (n = 1 or 2, L = PR_3) complexes. The variation in the Cu···Cu distance in these complexes was interpreted in the framework of the EHMO theory in terms of a direct electron density transfer from the orbitals of the bridging halide atoms, X, into the 4s and 4p orbitals of Cu, which is traced to weak σ and π Cu···Cu interactions. More recently, Alvarez et al.[26] have analyzed the effect of the halide ligand on Cu−Cu bonding in a series of complexes $[CuXL]_2$ (X = Cl, Br, I; L = NH_3, PH_3,CNMe) using MP2 and B3LYP computational techniques. They found that the Cu−Cu distance decreases upon increasing the size of the bridging halide ligand. The computed ∠X−Cu−X bond angles found in the range 101.4−116.4° increases by 5.4° and 9.9° along the series of the chloro, bromo, and iodo derivatives, respectively. On the other hand, the ∠Cu−X−Cu bond angles found in the range 78.9−63.7° follow the reverse order, decreasing by 5.4° and 9.8° along the series of the chloro, bromo, and iodo derivatives, respectively. Finally, the τ(P−P−Cu−X) dihedral angle defined by the P−Cu−P and X−Cu−X planes in the tetrahedral coordination sphere of each Cu(I) central atom found in the range 118.5−126.5° increases successively by about 4° along the series of the chloro, bromo, and iodo derivatives. The computed ν_{sym}(X−Cu−X) stretching vibrational frequencies appearing at 180, 125, and 95 cm^{-1}, for the $[Cu(\mu$-Cl)$(PH_3)_2]_2$, $[Cu(\mu$-Br)$(PH_3)_2]_2$, and $[Cu(\mu$-I)$(PH_3)_2]_2$ complexes, respectively, are compatible with the elongated Cu−X bonds in the dimers. The same holds true also for the ν_{sym}(Cu−X−Cu) stretching vibrational frequencies appearing at 225, 146, and 136 cm^{-1}, for the chloro, bromo, and iodo derivatives of the dimers, respectively. Obviously, both these bands could be used as a guide for distinguishing the dimers from their monomers.

Interestingly the dimerization of $CuX(PH_3)_2$ monomers does not tune the natural and net atomic charges on the Cu(I) metal centers and the bridging halide ligands as well. The Cu(I) metal centers acquire a positive natural charge of about 0.5−0.6 charge unit (0.2−0.3 charge unit of Mulliken net atomic charge), while the bridging halide ligands acquire a negative natural (Mulliken net atomic) charge of −0.70 (−0.36) to −0.75 (−0.44) charge unit. Notice that the natural electron configuration on the Cu(I) central atom and the halide ligands assigned by the NBO analysis (Table 7) is not affected significantly by the nature of the halide ligands. The most noticeable differences concern the iodo derivative and could probably be accounted for by the larger overlap between the orbitals used to built the Cu−X bonds in the rhombus of the $[Cu(\mu$-I$)(PH_3)_2]_2$ dimer compared to that of the other counterparts.

All $[Cu(\mu$-X$)(PH_3)_2]_2$ dimers exhibit a similar pattern of molecular orbital level diagram with a successive lowering of the respective eigenvalues on going from the chloro to bromo and to iodo derivatives. This is consistent with the higher stability of the $[Cu(\mu$-I$)(PH_3)_2]_2$ dimer in the series. The most important MOs of the $[Cu(\mu$-X$)(PH_3)_2]_2$ dimers are collected in Figure 7. Perusal of Figure 7 reveals that the Cu(μ-X)Cu moiety exhibits a composite bonding mode involving both σ and π components. The HOMO corresponding to a π* antibonding Cu−X interaction is strongly polarized toward the bridging halide ligands. On the other hand, the LUMO corresponds to a delocalized MO over the H atoms of the phospine ligands with a small contribution from a d orbital of the Cu(I) central atoms, as well. Noteworthy is the presence of π-type MOs delocalized over the entire four-membered Cu(μ-X)$_2$Cu ring similar to the π-type MOs of the cyclobutadiene molecule, which support a ring current. However, the Cu(μ-X)$_2$Cu ring, having a total of 8 framework electrons, does not obey the ($4n + 2$) Hückel rule to be an aromatic systems and thereby corresponds to an antiaromatic system. The delocalized π electron density in the Cu(μ-X)$_2$Cu rhombus could probably account for the nearly equivalent Cu−X bonds in the rhombus. Surprisingly, all $[Cu(\mu$-X$)(PH_3)_2]_2$ dimers exhibit a σ-type MO corresponding to weak intermetallic Cu···Cu interactions (Figure 7), which seems to be inconsistent with the relatively long Cu···Cu separation distances and the FEC (framework electron counting) rule introduced by Alvarez et al.[27] According to this rule it is the number of framework electrons that account for the through-ring bonding in edge-sharing dimers of square planar complexes. Thus, a short through-ring distance is predicted for compounds with FEC = 4 or 6, but a distance that is not short is expected for those with FEC = 8. Notice that the electron density in the region between the two bonded Cu atoms increases successively along the series of the chloro, bromo, and iodo derivatives in line with the computed Cu···Cu separation distances. On

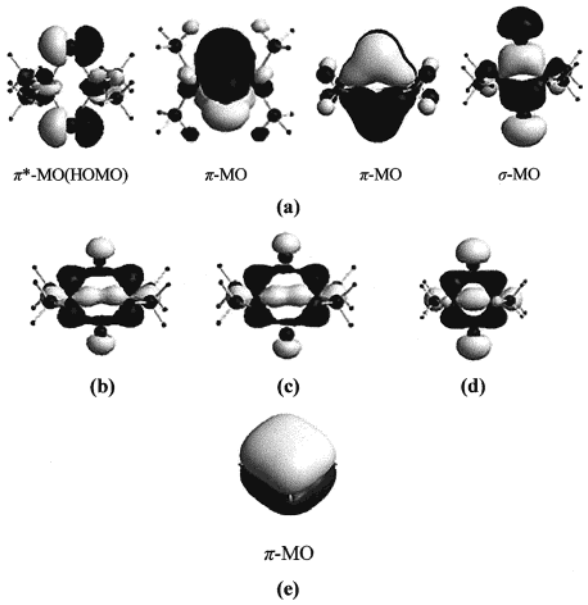

Figure 7. The most important MOs of the $[Cu(\mu$-X$)(PH_3)_2]_2$ dimers: HOMO, π- and σ-type MOs (a), σ-type Cu−Cu MO of the chloro (b), bromo (c), and iodo derivatives (d), and π-type MO of C_4H_4 (e).

(26) Carvajal, A.; Liu, X.-Y.; Alemany, P.; Novoa J. J.; Alvarez, S. *Int. J. Quantum Chem*. **2002**, 86, 100−105.

(27) Alemany, P.; Alvarez, S. *Inorg. Chem*. **1992**, *31*, 4266−4275.

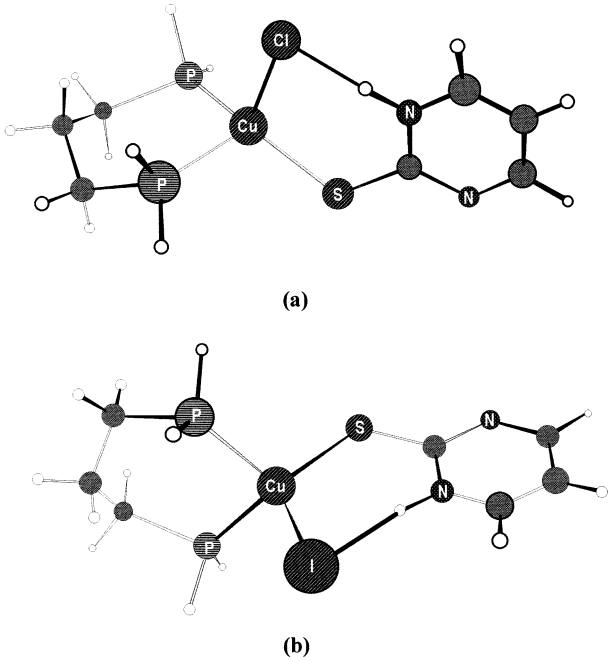

Figure 8. Equilibrium structures of the CuX(1,3-pdp)(pymtH) complexes computed at the B3LYP/SDD level of theory.

the other hand the computed negative *bop* values (Table 7) for the Cu···Cu interactions are indicative of antibonding interactions, but this might be an artifact of the Mulliken population analysis with its well-known shortcomings. In summary, the present computational results indicate that weak intermetallic Cu···Cu interactions are indeed present in $[Cu(\mu\text{-}X)(PH_3)_2]_2$ dimers probably as a correlation effect, in the framework of the B3LYP level of theory, being responsible for the stabilization of the otherwise unstable antiaromatic $Cu(\mu\text{-}X)_2Cu$ ring.

Equilibrium Geometry, Electronic Structure, and Bonding Mechanism in [CuX(PH$_3$)$_2$(pymtH)] and [CuX(1,3-pdp)(pymtH)] (X = Cl, Br or I) Compounds. The details of the structural, energetic, and electronic properties of the [CuX(PH$_3$)$_2$(pymtH)] and [CuX(1,3-pdp)(pymtH)] (X = Cl, Br, or I; pymtH = pyrimidine-2-thione) complexes have also been explored at the B3LYP/SDD level of theory. Representative fully optimized equilibrium geometries of the [CuX(1,3-pdp)(pymtH)] compounds along with the atom-labeling scheme are shown in Figure 8. Selected structural parameters for the [CuX(PH$_3$)$_2$(pymtH)] and [CuX(1,3-pdp)(pymtH)] compounds along with their total electronic energies, dipole moments, and some electronic properties are compiled in Tables 8 and 9, respectively. In general terms the optimized geometries of the [CuX(1,3-pdp)(pymtH)] compounds resemble those determined experimentally by X-ray crystallography. All these compounds involve a four-coordinated Cu(I) central atom in a tetrahedral coordination environment with the plane of the thione ring coinciding with the line bisecting the ∠P−Cu−P angle. Interestingly, the conformation of the thione ligand is further stabilized through an X···H interaction (H-bond formation). The computed X···H distances in CuX(PH$_3$)$_2$(pymtH) compounds are 2.026, 2.200, and 2.451 Å for the chloro, bromo, and iodo derivatives, respectively, whereas those in [CuX(1,3-pdp)(pymtH)] compounds are 2.024, 2.200, and 2.405 Å. The H-bond formation is also reflected in the computed *bop* values for the respective interactions as well as in the existence of a molecular orbital having a strong σ component corresponding to the X···H interactions (Figure 9). The strength of the H-bonds formed is tuned by the identity of the halide ligand following the expected order: Cl > Br > I. The H-bond formation introduces a small lengthening of the N−H bond in the pymtH ligand, its length being 1.054, 1.048, and 1.043 Å for the chloro, bromo, and iodo derivatives, respectively. The X···H−N moiety is nearly linear, with the computed ∠X···H−N bond angle found in the range 172.7−176.6°. In both series of complexes the linearity of the X···H−N moiety

Table 8. Selected Structural Parameters, Total Energies, and Electronic Properties of CuX(PH$_3$)$_2$(pymtH) (X = Cl, Br, I) Compounds Computed at the B3LYP/SDD Level of Theory

	CuCl(PH$_3$)$_2$-(pymtH)	CuBr(PH$_3$)$_2$-(pymtH)	CuI(PH$_3$)$_2$-(pymtH)
E (hartrees)	−2006.18170	−1559.37896	−1557.41601
R_e(Cu−X) (Å)	2.417	2.550	2.731
R_e(Cu−P) (Å)	2.377	2.383	2.386
R_e(Cu−S) (Å)	2.441	2.435	2.431
θ_e(S−Cu−X) (deg)	113.0	114.9	118.9
θ_e(P−Cu−X) (deg)	102.7	103.5	101.9
θ_e(P−Cu−S) (deg)	108.9	108.0	108.1
θ_e(P−Cu−P) (deg)	120.2	119.2	118.5
τ(P−P−Cu−X) (deg)	113.5	114.1	110.7
μ_e (D)	1.13	1.33	2.04
η (eV)	1.614	1.619	1.537
q_{Cu}[a]	0.55 (0.15)[b]	0.55 (0.17)	0.52 (0.14)
q_X	−0.72 (−0.44)	−0.74 (−0.51)	−0.71 (−0.50)
q_S	−0.26 (0.08)	−0.26 (0.08)	−0.25 (0.09)
bop(Cu−X)[c]	0.235	0.166	0.166
bop(Cu−S)	0.224	0.245	0.244
nec(Cu)[d]	$4s^{0.49}3d^{9.88}$	$4s^{0.49}3d^{9.90}$	$4s^{0.53}3d^{9.91}$
nec(X)	$4s^{1.97}3d^{5.76}$	$4s^{1.97}3d^{5.78}$	$4s^{1.97}3d^{5.73}$
nec(S)	$4s^{1.97}3d^{5.76}$	$4s^{1.97}3d^{5.78}$	$4s^{1.97}3d^{5.73}$

[a] Natural charges. [b] Figures in parentheses are the Mulliken net atomic charges. [c] Mulliken bond overlap population. [d] Natural electron configuration.

Table 9. Selected Structural Parameters, Total Energies, and Electronic Properties of CuX(1,3-pdp)(pymtH) (X = Cl, Br, I) Compounds Computed at the B3LYP/SDD Level of Theory

	CuCl(1,3-pdp)-(pymtH)	CuBr(1,3-pdp)-(pymtH)	CuI(1,3-pdp)-(pymtH)
E (hartrees)	−2123.05869	−1676.25633	−1674.29264
R_e(Cu−X) (Å)	2.408	2.556	2.722
R_e(Cu−P) (Å)	2.386	2.390	2.395
R_e(Cu−S) (Å)	2.408	2.395	2.405
θ_e(S−Cu−X) (deg)	114.0	116.6	119.4
θ_e(P−Cu−X) (deg)	107.1	104.5	105.9
θ_e(P−Cu−S) (deg)	115.1	116.0	113.1
θ_e(P−Cu−P) (deg)	96.9	96.8	96.8
τ(P−P−Cu−X) (deg)	110.3	106.9	108.7
μ_e (D)	1.60	1.77	2.32
η (eV)	1.538	1.533	1.456
q_{Cu}[a]	0.56 (0.01)[b]	0.55 (0.04)	0.52 (0.02)
q_X	−0.72 (−0.45)	−0.74 (−0.52)	−0.71 (−0.51)
q_S	−0.25 (0.07)	−0.24 (0.09)	−0.24 (0.09)
bop(Cu−X)[c]	0.231	0.141	0.146
bop(Cu−S)	0.217	0.239	0.237
nec(Cu)[d]	$4s^{0.49}3d^{9.90}$	$4s^{0.50}3d^{9.90}$	$4s^{0.52}3d^{9.91}$
nec(X)	$4s^{1.96}3d^{5.76}$	$4s^{1.97}3d^{5.77}$	$4s^{1.97}3d^{5.74}$
nec(S)	$4s^{1.77}3d^{4.46}$	$4s^{1.77}3d^{4.46}$	$4s^{1.77}3d^{4.46}$

[a] Natural charges. [b] Figures in parentheses are the Mulliken net atomic charges. [c] Mulliken bond overlap population. [d] Natural electron configuration.

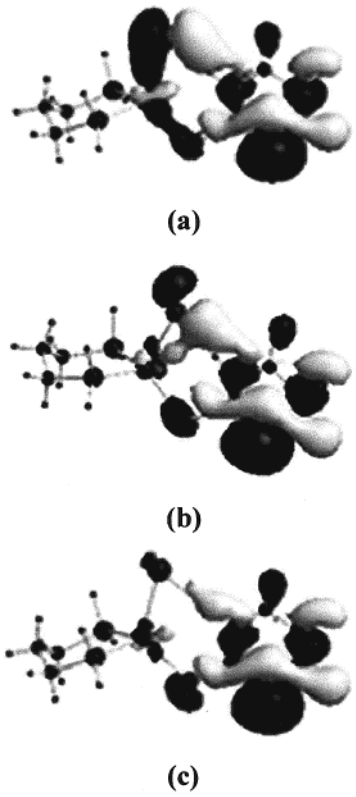

Figure 9. The σ-type MOs corresponding to the X···H−N interactions in the chloro (a), bromo (b), and iodo derivatives (c) of the CuX(1,3-pdp)-(pymtH) complexes.

decreases from the chloro to bromo and to iodo compounds. Moreover, in both series of complexes the ∠Cu−X−H bond angle, found in the range 74.4−110.1°, decreases successively by about 5° from the chloro to bromo and to iodo derivatives. However, the opposite holds true for the ∠S−Cu−X and ∠Cu−S−C bond angles.

Upon coordination of the thione ligand with the Cu(I) metal center in the $[CuX(PH_3)_2]$ and [CuX(1,3-pdp)] complexes, no significant structural changes are observed in the heterocycle ring of thione. However, in both series of complexes the coordination of thione through the S donor atom of the C═S group results in an elongation of the C═S bond by 0.037 Å. This might be the result of the transfer of electron density from the C═S group to the Cu(I) metal center upon formation of the coordination Cu−S bond through the interaction of the HOMO of thione, being a π-type MO localized on the C═S group (Figure 10), with a vacant orbital of the central atom. There is also a possibility for π-back-bonding through the interaction of an occupied orbital of the central Cu(I) atom with the LUMO of the thione ligand, being a π*-type MO delocalized over the entire nuclear skeleton of the thione ligand. The π-back-bonding effect is clearly illustrated by the presence of the appropriate MO (Figure 10b) in all complexes of the two series. In spite of the composite nature of the Cu−S coordination bond, exhibiting both a σ and a π component, the bond is relatively weak, the computed bond dissociation energy predicted to be 22.7, 20.8, and 19.2 kcal/mol for the chloro, bromo, and iodo derivatives, respectively, at the B3LYP/SDD level of theory. The weaker Cu−S coordination bond in the iodo

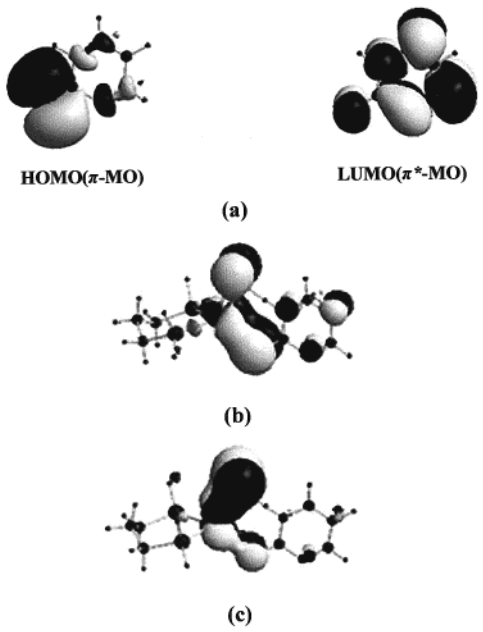

Figure 10. The HOMO and LUMO of the pymtH ligand (a) along the MOs corresponding to the π bonding component of the Cu−S (b) and Cu−X (c) interactions.

derivatives in conjunction with the weaker H-bond formation could account well for the preference of the iodo monomers to form dimers rather than to be coordinated with the thione ligand.

The Cu−X bond also exhibits a partially double bond character analogous to that found in the $[CuX(PH_3)_2]$ and [CuX(1,3-pdp)] monomers. A representative π-type MO localized on the Cu−X bond is shown in Figure 7c. It can be seen that the Cu−X bonds are elongated by approximately 0.2 Å upon coordination of the thione ligand to the $[CuX(PH_3)_2]$ and [CuX(1,3-pdp)] complexes. The elongation of the Cu−X bond is reflected on the computed bond overlap populations found in the range 0.141−0.235 in the complexes as compared to the *bop*(Cu−X) values of the $[CuX(PH_3)_2]$ and [CuX(1,3-pdp)] species (Tables 5 and 6). Similarly, the elongation of the C═S bond is reflected on the computed bond overlap populations found in the range 0.269−0.285 in the complexes as compared to the *bop*(C−S) value of 0.422 in the free thione ligand. Noteworthy is the transfer of electron density from the S donor atom of the thione ligand to the halide ligand, assisted by the Cu(I) central atom. Overall, there are no remarkable changes in both the natural and net atomic charges of the donor (P, X) and central (Cu) atoms in the $[CuX(PH_3)_2$(pymtH)] and [CuX(1,3-pdp)-(pymtH)] compounds as compared to those of the precursor $[CuX(PH_3)_2]$ and [CuX(1,3-pdp)] complexes. The same holds true also for the natural electron configurations of the respective atoms, which seem to be insensitive to the identity of both the phosphine and halide ligands. This strongly supports our finding that the interaction of the thione ligand with the closed-shell d^{10} Cu(I) metal center in a variety of coordination environments is very weak, the computed interaction energy predicted to be approximately 20 kcal/mol. It seems that H-bond formation and other types of

intermolecular forces might be of key importance in stabilizing the coordination of thione ligands with the Cu(I) central atom.

Finally, the computed ν(Cu-X) vibrational frequencies appearing at 208, 160, and 127 cm^{-1}, for the chloro, bromo, and iodo derivatives of the [$CuX(PH_3)_2$(pymtH)] complexes, respectively, are compatible with the computed Cu−X bond lengths. The ν(Cu−S) vibrational frequencies were found at 170, 162, and 161 cm^{-1} for the chloro, bromo, and iodo derivatives of [$CuX(PH_3)_2$(pymtH)] complexes, respectively. Notice that the previous tentative assignment of the band of medium intensity in the region of 340−370 cm^{-1} to the ν-(Cu−S) vibrational mode[28] seems to be incorrect, as this band is predicted to occur at much lower frequencies. The ν(Cu−P) vibrational modes are predicted to absorb in the region of 205−208 cm^{-1}. The ν(C−S) vibrational frequency calculated to be 455 cm^{-1} for all complexes of the series is shifted to much lower frequencies than the corresponding band of the free pymtH ligand found at 734 cm^{-1}. The computed ν(C−S) vibrational frequencies are in line with the computed C−S bond lengths, being exactly the same for all complexes in the series, but remarkably elongated with respect to the free pymtH ligand. Of particular importance is the ν(N−H) stretching vibrational mode appearing at 2974, 3033, 3110, and 3591 cm^{-1} in the [$CuCl(PH_3)_2$(pymtH)], [$CuBr(PH_3)_2$(pymtH)], and [$CuI(PH_3)_2$(pymtH)] complexes and the free pymtH, ligand, respectively. It can be seen that there is a strong shift of the ν(N−H) vibrational frequencies to much lower values upon coordination of the ligand with the Cu(I) metal center. The shifting of the ν(N−H) vibrational frequencies to lower frequencies is indicative of the involvement of the H atom in H-bond formation with the halide ligand and reflects the relative strength of the X···H−N bond formed.

Conclusions

In this work we report on the coordination behavior of Cu(I) chloride, bromide, and iodide in the presence of a series of heterocyclic thiones and 1,3-propanebis(diphenylphosphine) as ligands. In all the complexes, 1,3-propanebis(diphenylphosphine) acts as a bidentate ligand forming stable six-membered chelate rings, whereby the neutral thione ligands adopt the monodentate coordination mode binding the Cu(I) center through the exocyclic sulfur atom. Nevertheless, depending on the nature of the halide ligands, two different types of compounds, namely, monomeric with tetrahedrally coordinated Cu(I) for X = Cl and Br and dimeric with double-bridging iodo ligands for X = I, have been isolated, even under the same reaction conditions. Although within this class of mixed-ligand complexes we often observed such a dimerization, it is remarkable that the strong tendency of copper(I) to bind the "soft" iodide ligands enforces, in the present case, the exclusion of the thione ligand from the coordination sphere. This could be supported by the presence of the diphosphine ligand and its strong chelating effect. However, similar results are obtained using 1,5-pentanebis(diphenylphosphine), which does not act as a chelating agent but bridges the two metal centers in the dimer. Consequently, this phenomenon needs a more extensive study; therefore further examples of this series of compounds will be examined in the future.

According to the results of the DFT calculations the interaction of the thione ligand with the Cu(I) central atom corresponds to loose associations, the interaction energies predicted to be about 20 kcal/mol for all complexes in the series. The bonding mechanism of the thione ligand with the Cu(I) central atom involves both σ-dative and π-back-bonding components. The contribution of each component to the bonding mechanism is not affected by the identity of the phosphine and the halide ligands. The coordination of the thione ligand is further stabilized by X···H−N bond formation being more pronounced in the chloro than in the iodo derivatives. Similarly, the Cu−X bond in all complexes of the series involves both σ- and π-dative bonding components. However, most important is the presence of π-type MOs delocalized over the entire four-membered Cu(μ-X)$_2$Cu ring, supporting a ring current and probably accounting for the nearly equivalent Cu−X bonds in the rhombus. Moreover, all [Cu(μ-X)$(PH_3)_2]_2$ dimers exhibit a σ-type MO corresponding to weak through-ring intermetallic Cu···Cu interactions (d−d interactions), which seems to be responsible for the stabilization of the relatively unstable antiaromatic Cu(μ-X)$_2$Cu ring. Finally, the preference of the iodo monomers to afford dimers rather than to be coordinated with the thione ligand could be attributed both to the weaker Cu−S coordination bond in conjunction with the weaker X···H−N interactions as compared to those of the chloro and bromo monomers and to the higher stability of the [Cu(μ-I)$(PH_3)_2]_2$ dimers as compared to the chloro and bromo counterparts.

Acknowledgment. We thank the EPSRC X-ray crystallography service in the University of Southampton for collecting the X-ray data.

Supporting Information Available: Crystallographic data in CIF format. This material is available free of charge via the Internet at http://pubs.acs.org.

IC025896I

(28) Belamy, L. J. *The Infrared spectra of Complex molecules*; Wiley: New York, 1966.